

Self-referenced method for the Judd–Ofelt parametrisation of the Eu^{3+} excitation spectrum

Aleksandar Ciric

University of Belgrade, Vinca Institute of Nuclear Sciences

Lukasz Marciniak

Institute of Low Temperature and Structure Research

Miroslav Dramicanin (✉ dramican@gmail.com)

University of Belgrade <https://orcid.org/0000-0003-4750-5359>

Article

Keywords: Judd–Ofelt parametrisation, Eu^{3+} excitation, lanthanide luminescence, phosphors

Posted Date: September 27th, 2021

DOI: <https://doi.org/10.21203/rs.3.rs-934321/v1>

License: © ⓘ This work is licensed under a Creative Commons Attribution 4.0 International License.

[Read Full License](#)

Self-referenced method for the Judd–Ofelt parametrisation of the Eu^{3+} excitation spectrum

Aleksandar Ćirić^{a}, Łukasz Marciniak^b, and Miroslav D. Dramićanin^{a*}*

*^aVinča Institute of Nuclear Sciences – National Institute of the Republic of Serbia,
University of Belgrade, P.O. Box 522, Belgrade 11001, Serbia*

*^bInstitute of Low Temperature and Structure Research, PAS, ul. Okólna 2, 50-422 Wrocław,
Poland*

**Corresponding authors: aleksandar.ciric@ff.bg.ac.rs, dramican@vin.bg.ac.rs*

Abstract: Judd-Ofelt theory presents a centrepiece in spectroscopy of lanthanides since it explains and predicts 4f absorptions and emissions from only 3 intensity parameters. A self-referenced method for calculating Judd–Ofelt intensity parameters from the excitation spectra of Eu^{3+} -activated luminescent materials is proposed in this study along with a description of the parametrisation procedure and free user-friendly web application. It uses the integrated intensities of the ${}^7\text{F}_0 \rightarrow {}^5\text{D}_2$, ${}^7\text{F}_0 \rightarrow {}^5\text{D}_4$, and ${}^7\text{F}_0 \rightarrow {}^5\text{L}_6$ transitions in the excitation spectrum for calculations and the integrated intensity of the ${}^7\text{F}_0 \rightarrow {}^5\text{D}_1$ magnetic dipole transition for calibration. This approach allows a simple derivation of the Ω_6 intensity parameter, which is difficult to calculate precisely by Krupke’s parametrisation of the emission spectrum and, therefore, frequently omitted in published research papers. Compared to the parametrisation of

absorption spectra, the described method is more accurate, can be applied to any material form, and requires a single excitation spectrum.

Keywords: Judd–Ofelt parametrisation, Eu^{3+} excitation, lanthanide luminescence, phosphors

1. Introduction

Lanthanides have revolutionised the modern science and technology and are present in almost any device¹. The global value of lanthanide-containing products estimated in 2014 was 1.5–2 trillion dollars², and this number has been continuously increasing since that time. Moreover, the use of lanthanides in phosphors accounts for approximately 3% of the total market share¹. Considering lanthanide applications in phosphors, researchers focus on luminescent properties, which make these compounds unique among other luminescence centres. Owing to the characteristic electronic configuration of trivalent lanthanide ions, their luminescence due to $4f-4f$ electronic transitions is characterised by the narrow emission and absorption bands, host-independent transition energies, and plethora of emissions spanning across the ultraviolet–near infrared (NIR) spectral range with long emission decays and high quantum efficiencies³.

From the viewpoint of the quantum theory developed in the 1920–1930s, the spectral properties of lanthanides were puzzling as summarised by Van Vleck in his famous article 'The Puzzle of Rare-earth Spectra in Solids' published in 1937⁴. In particular, the high intensities of intra-configurational $4f$ transitions contradicted the parity (Laporte) selection rule⁵. Owing to development of Racah's algebra in 1949 and first computers allowing the tabulation of many required coefficients, two equivalent articles were published almost simultaneously in 1962 by

Judd in *Physical Review*⁶ and Ofelt in *The Journal of Chemical Physics*⁷ which were characterised by B. Wybourne in the following words⁸:

'The two papers of 1962 represent the paradigm that has dominated all future work...up to the present time'

What was later coined as the Judd–Ofelt theory (JO) provided the first quantum-mechanical explanation of the intensities of induced electric dipole transitions. The centrepiece of this theory includes three intensity parameters Ω_λ , $\lambda = 2, 4, 6$, from which many ‘derived quantities’ with high practical importance (such as radiative transition probabilities, radiation lifetimes, branching ratios, cross-sections, and intrinsic quantum yields) can be simply obtained. These parameters may be subsequently used to calculate the intensities of the entire emission or absorption spectra⁹.

Considering the capability of the JO theory and spectroscopic importance of lanthanides, it is not surprising that the research interest in this theory is rapidly growing (Figure 1).

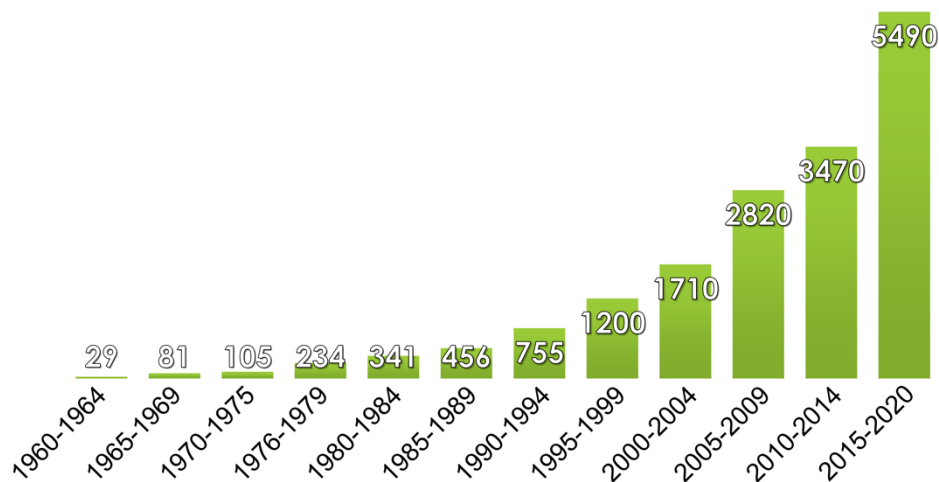


Figure 1 Numbers of published papers with the expression “Judd–Ofelt” determined for 5-year intervals by Google Scholar (accessed in July 2021).

The ongoing research studies in this field can be classified into three categories: (i) theory improvement and development of alternate JO parametrisation methods^{5,10–17}, (ii) JO parametrisation of lanthanides in different hosts doped at various concentrations and analysis of lanthanide-activated phosphors synthesised by different methods (see Tables 10–21 in Ref.¹⁸), and (iii) applications of JO theory and JO parameters by constructing various models in other areas of science related to luminescence^{19,20}. The majority of research works on these topics fall into categories (ii) and (iii), demonstrating that the practical implementation of the JO theory does not require its deep understanding. For category (ii), it is necessary to know the methods for calculating JO parameters, while for research category (iii), such parameters can be obtained from the literature.

2. Previous JO parametrisation studies

JO parameters are traditionally determined by analysing the absorption spectra of trivalent lanthanide-activated materials. This method is described in detail in Refs.^{5,9}; therefore, only its brief description is provided below. It is based on fitting the experimental oscillator strengths obtained from the absorption spectrum with theoretical equations derived for selected transitions of a given lanthanide ion. The experimental oscillator strength (P_{exp}) is equal to¹⁸

$$P_{exp}[f] = 4.32 \cdot \frac{10^{-9}\Xi}{X_A}, \quad (1)$$

where

$$\Xi = \int \varepsilon(\nu) d\nu, \quad (2)$$

is the integrated molar absorptivity, ν is the wavenumber [cm^{-1}], and X_A is the fractional thermal population at the initial level. ε [$\text{mol}^{-1} \text{L cm}^{-1}$] is the molar extinction coefficient (molar absorptivity), which can be calculated from absorbance by the following formula:

$$\varepsilon = Cd/A. \quad (3)$$

Here, C [mol/L] is the concentration, and d [cm] is the length of the optical path in a given material.

At temperatures above the absolute zero, the higher-lying energy levels of lanthanide ions are thermally populated with probabilities specified by the Boltzmann distribution. If the energy separation to the next level is larger than 2000 cm^{-1} , the thermalisation of the current energy level is not efficient and may not follow the Boltzmann distribution (in this case, it can be even neglected due to its low contribution). The ratio of the optical centres at a selected level to the total number of optical centres is represented by the fractional thermal population^{18,21}:

$$X_A = \frac{g_A \exp\left(-\frac{\Delta E_A}{kT}\right)}{\sum_i g_i \exp\left(-\frac{\Delta E_i}{kT}\right)}, \quad (4)$$

where T [K] is the temperature, g_i is the level of degeneracy, ΔE_i is the energy difference between level i and the ground state (in cm^{-1}), and $k = 0.695 \text{ cm}^{-1} \cdot \text{K}^{-1}$ is the Boltzmann constant. According to the fractional thermal population of the Eu^{3+} ground multiplet ${}^7\text{F}_J$, the ${}^7\text{F}_1$ level is significantly populated even at room temperature due to the low energy separation between the ${}^7\text{F}_{0,1}$ levels, which can be verified by the excitation or absorption spectra that contain transitions originating from the $\text{Eu}^{3+} {}^7\text{F}_1$ level²².

Unlike the oscillator strength, dipole strength is independent of the photon energy and related to the oscillator strength via the following expression:

$$P_{\text{th}} [/\text{}] = 4.702 \cdot 10^{29} \tilde{\nu} D_{\text{th}}, \quad (5)$$

where $\tilde{\nu}$ is the transition barycentre energy (in cm^{-1}), and D_{th} is the dipole strength. The dipole strength of the electric dipole (ED) transition is defined as⁹

$$D_{\text{th}}^{\text{ED}} [\text{esu}^2 \text{cm}^2] = e^2 \sum_{\lambda} \Omega_{\lambda} U^{\lambda}, \quad (6)$$

where U^{λ} are the squared reduced matrix elements (RMEs), and $e = 4.803 \cdot 10^{10}$ esu is the elementary charge. RMEs are often considered host-independent; for this reason, many researchers have resorted to using the values tabulated by Carnall et al.²³ instead of calculating them for a particular host by employing Slater integrals and spin-orbit coupling parameters²⁴. The magnetic dipole (MD) transition has a dipole strength that is also host-independent. The tabulated values for all MD transitions of all trivalent lanthanides are provided in Ref.²⁵.

The experimental oscillator strength is compared to the theoretical strength by the formula

$$P_{\text{exp}} = \frac{\chi}{g} P_{\text{th}}, \quad (7)$$

where χ is the local field correction, and $g = 2J + 1$ is the degeneracy of the J level, from which the transition originates. The Lorenz field correction for the ED transition and local field correction for the MD transition during absorption are computed as follows²⁶:

$$\chi_{\text{ED}}^{\text{ab}} = \frac{(n^2 + 2)^2}{9n}, \quad \chi_{\text{MD}}^{\text{ab}} = n, \quad (8)$$

where n is the wavelength-dependent refractive index. Ideally, the refractive index is calculated using the dispersion relation.

To obtain JO parameters, all P_{exp} magnitudes should be fitted to P_{th} using Eq. (7) for the observed transitions, thereby minimising the discrepancies between the theoretical and

experimental values. Ultimately, this will produce Ω_λ values closest to the experimental data. As pointed out by Blasse and co-workers, a drawback of this method is the necessity to accurately measure the density of ions in the analysed sample. In addition, absorption intensity can be routinely measured only for glasses, transparent solutions, and crystals, leaving out non-transparent materials and crystalline powders¹³. Another drawback of the described approach is a high error of $\sim 20\%$ ²⁷ caused by the absence of higher-order contributions, whose inclusion significantly complicates the calculation procedure (see Ref.²⁸). The third problem arises with the parametrisation of the Pr^{3+} ion as the proximity of the $4f5d$ levels mixes with the $4f$ levels, leading to a case that cannot be treated by the original JO method. As a result, complex alternative parameterisation methods with questionable accuracies were developed for Pr^{3+} ions¹¹. Parametrisation using crystal field parameters is called *ab initio* parameterisation; however, it suffers from high complexity and limited accuracy, as stated by L. Smentek¹⁰:

‘Indeed, there are objective, or rather technical reasons, why it is still impossible to perform ab initio calculations that would provide reliable results.’

The readers interested in this method are referred to Refs.^{18,29,30}.

Various techniques similar to the absorption-based one, which utilise excitation¹⁵ or diffuse-reflectance³¹ spectra, have been proposed in recent years. Their development was motivated by the limited application of the absorption method for powders and non-transparent materials. Although these techniques can be used for any material, they produce only relative JO parameters, which must be calibrated against the radiative transition probability of a selected level that is approximately equal to the experimentally measured lifetime. This assumption inherently introduces an error into the calculated values. For this reason, the authors of both the

above-mentioned methods have chosen the first excited level of Er^{3+} for the calibration by the excited-level lifetime value (because it is almost purely radiative) and Nd^{3+} ion for the diffuse-reflectance method. However, their applicability to other lanthanide ions has not been tested or theoretically verified.

Sytsma and Blasse were the first researchers who performed spectrum calibration using an excited-level lifetime for the JO parametrisation of the Gd^{3+} emission spectrum¹³ assuming that the deexcitation of its first excited level, which lied high above the ground level, was purely radiative. A similar approach was explored in our previous research study¹² describing a JO parametrisation method that utilised the Pr^{3+} emission spectrum. Because the emissive $^3\text{P}_0$ level is non-degenerate, parametrisation can be performed using the low-temperature emission spectrum with negligible temperature quenching. At low Pr^{3+} concentrations, the depopulation of the excited states through the interionic processes was very small, and the radiative lifetime of the $^3\text{P}_0$ level was equal to the experimentally measured value. This allowed conducting more accurate spectrum calibration and JO parameterisation than the corresponding procedures of the alternative absorption methods mentioned above.

In 1966, shortly after Judd and Ofelt had published their articles, Krupke developed a JO parametrisation method using the emission spectrum of the Eu^{3+} ion¹⁷. Because this method includes the higher-order contributions not considered in the traditional parametrisation of the absorption spectrum, it remains the most accurate JO parameterisation technique. Unlike the methods that require calibration with the excited level lifetime, Krupke exploited the fact that Eu^{3+} had a pure host-independent MD transition $^5\text{D}_0 \rightarrow ^7\text{F}_1$, to which other intensities could be compared. In the method proposed in our previous work¹⁶, the pure MD $^5\text{D}_1 \rightarrow ^7\text{F}_0$ emission is used for spectral calibration and, as will be demonstrated later, the same energy levels are

utilised in the novel parametrisation technique developed in this study. Owing to the use of an accurate dispersion relation for the refractive index, the JO parameterisation methods based on the emission spectra of the Eu^{3+} ion are unbeatable in terms of accuracy and simplicity. However, in such spectra, the only transition that can be used to calculate the Ω_6 parameter lies in the NIR region outside the detection limits of most traditional detectors and is also very weak due to the low $U^6 = 0.0002 \text{ RME}^{32}$. Only a limited number of studies have reported the ${}^5\text{D}_0 \rightarrow {}^7\text{F}_6$ emission^{33–37}. Thus, JO parameterisations performed using Eu^{3+} emission spectra are often incomplete. Furthermore, because U^6 has a low value, it is estimated with relatively large error and variations^{32,38}, making the parameterisation of the Ω_6 value based on the emission spectrum unreliable and difficult to perform. Despite its low importance for Eu^{3+} emission, Ω_6 is the most important parameter in the absorption/excitation spectrum, as the most intense absorption, ${}^7\text{F}_0 \rightarrow {}^5\text{L}_6$, depends solely upon its value. The Ω_6 magnitude is related to the rigidity of a medium where ions are incorporated^{39,40}, which in turn depends on the Debye temperature^{41,42}. Consequently, there is experimental and theoretical incompleteness of the JO parametrisation of Eu^{3+} -activated materials that are not glasses, crystals, or solutions.

Self-calibrated JO parametrisation of the Eu^{3+} excitation spectrum (JOEX)

Therefore, to perform accurate JO parameter determination and avoid the limitations of the methods described above, we propose a novel technique for the JO parametrisation of Eu^{3+} -doped materials, which enables the estimation of all three Ω_λ parameters from a single excitation spectrum. Unlike the other methods that rely on spectrum calibration by the excited-level lifetime, this approach utilises the pure MD transition ${}^7\text{F}_0 \rightarrow {}^5\text{D}_1$ at 525 nm for calibration purposes. The proposed method simultaneously facilitates the determination procedure and increases the reliability of the obtained results. The versatility of this technique allows its

application to non-transparent and powder materials, for which other methods are not suitable. It includes all higher-order contributions to the JO parameters (the original absorption spectrum-based method utilised only a static coupling model)⁴³. Owing to the high U^6 value obtained for the ${}^7F_0 \rightarrow {}^5L_6$ electronic transition of Eu^{3+} ions, U^6 was used with low relative uncertainty. In addition, due the high intensity of the band associated with the ${}^7F_0 \rightarrow {}^5L_6$ transition, its integrated intensity was also estimated with low uncertainty, contrary to the ${}^5D_0 \rightarrow {}^7F_6$ emission in Krupke's method.

In order to verify the reliability of the data obtained by the proposed method, the latter was applied to two different (from the chemical and morphological perspectives) materials: well-known Eu^{3+} -activated Y_2SiO_5 microcrystalline phosphor and $\beta\text{-NaYF}_4$ nanoparticles. The determined parameters were compared with the results obtained by Krupke's parametrisation technique and the emission spectrum calculated by the JOES application software (<https://omasgroup.org/joes-software/>)⁴⁴.

3. Theoretical approach

The experimental dipole strength of a randomly oriented system (e.g., powder) in its absorption spectrum is equal to¹⁸

$$D_{\text{exp}}[\text{esu}^2\text{cm}^2] = \frac{\text{E}}{108.9 \cdot 10^{36} \tilde{\nu} X_A}. \quad (9)$$

The experimentally obtained dipole strength can be compared with the theoretical value using the formula

$$D_{\text{exp}} = \frac{\chi}{g} D_{\text{th}}. \quad (10)$$

These equations are suitable for both ED and MD transitions; therefore, local field corrections must be applied accordingly. For pure MD and ED transitions, equation (10) can be modified as follows:

$$\frac{\Xi_{MD}}{108.9 \cdot 10^{36} \tilde{\nu}_{MD} X_A^{MD}} = \frac{\chi_{MD}}{g_{MD}} D_{MD}^{th}, \quad (11)$$

$$\frac{\Xi_{ED}}{108.9 \cdot 10^{36} \tilde{\nu}_{ED} X_A^{ED}} = \frac{\chi_{ED}}{g_{ED}} e^2 \sum_{\lambda} \Omega_{\lambda} U^{\lambda}. \quad (12)$$

In the case of the $4f-4f$ lanthanide transitions, the excitation spectrum is assumed to be identical to the corresponding absorption spectrum multiplied by a constant. Because absolute values cannot be obtained from excitation spectra, only cD_{exp} may be calculated via equation (9) as follows:

$$cD_{\text{exp}} [\text{esu}^2 \text{cm}^2] = \frac{\Gamma}{108.9 \cdot 10^{36} \tilde{\nu} X_A}, \quad (13)$$

where $\Gamma = c\Xi$ is the integrated intensity in the excitation spectrum for the corresponding transition, which is equal to the integrated molar absorptivity multiplied by the unknown c coefficient. Thus, the knowledge of c would allow JO parameterisation using equation (12). For the pure Eu^{3+} ED transitions ${}^7F_0 \rightarrow {}^5D_4$ ($\lambda = 4$), ${}^7F_0 \rightarrow {}^5L_6$ ($\lambda = 6$), and ${}^7F_0 \rightarrow {}^5D_2$ ($\lambda = 2$), the theoretical dipole strength can be expressed as

$$D_{\lambda} = e^2 \Omega_{\lambda} U^{\lambda}, \quad (14)$$

considering that all RMEs other than U^{λ} are equal to zero (see Table 1). In this case, equation (13) becomes

$$\frac{\Gamma_{\lambda}}{108.9 \cdot 10^{36} \tilde{\nu}_{\lambda} X_A({}^7F_0)} = c \chi_{\lambda} e^2 \Omega_{\lambda} U^{\lambda}. \quad (15)$$

Note that the degeneracy term is absent from this formula because $J = 0$ for the initial level.

Table 1. RMEs of various transitions relevant for the JO parametrisation of the Eu^{3+} excitation spectrum.

Transition	U²	U⁴	U⁶
${}^7\text{F}_0 \rightarrow {}^5\text{D}_2$	0.0009	0	0
${}^7\text{F}_0 \rightarrow {}^5\text{D}_4$	0	0.0011	0
${}^7\text{F}_0 \rightarrow {}^5\text{L}_6$	0	0	0.0153

In our recent article [16], we exploited the pure MD emission ${}^5\text{D}_1 \rightarrow {}^7\text{F}_0$ with an MD strength of $1.8 \cdot 10^{-42} \cdot \text{esu}^2 \cdot \text{cm}^2$. Because the dipole strength values determined for the emission and absorption/excitation processes are identical, the same dipole strength holds for the ${}^7\text{F}_0 \rightarrow {}^5\text{D}_1$ transition (further abbreviated as D_{MD}). As a result, equation (13) for the MD transition can be written in the following form:

$$\frac{\Gamma_{\text{MD}}}{108.9 \cdot 10^{36} \tilde{\nu}_{\text{MD}} \chi_A({}^7\text{F}_0)} = c \chi_{\text{MD}} D_{\text{MD}}. \quad (16)$$

After dividing equation (15) by equation (16), the fractional level populations vanish because the initial levels for calibrating the MD and ED transitions are the same. The unknown c parameter also disappears from the equation. As a result, a set of three equations for the determination of the JO parameters from the excitation spectrum is obtained:

$$\Omega_\lambda [\text{cm}^2] = \frac{\chi_{\text{MD}} \tilde{\nu}_{\text{MD}} D_{\text{MD}} \Gamma_\lambda}{\chi_\lambda \tilde{\nu}_\lambda e^2 U^\lambda \Gamma_{\text{MD}}}, \quad \lambda = 2, 4, 6. \quad (17)$$

Note that a similar equation can be derived by using the ${}^7\text{F}_1 \rightarrow {}^5\text{D}_0$ pure MD transition with a dipole strength $9.56 \cdot 10^{-42} \text{ esu}^2 \text{ cm}^2$ [25], but it would require the inclusion of degeneracies and fractional thermal populations.

4. Parametrisation procedure

A straightforward algorithm for obtaining JO intensity parameters from the excitation spectrum of Eu^{3+} is outlined below.

1. The excitation spectra of Eu^{3+} -activated materials can be obtained by monitoring the emission from the $^5\text{D}_0$ level (from 350 to 550 nm). Monitoring the $^5\text{D}_0 \rightarrow ^7\text{F}_2$ emission at approximately 612 nm is the best option due to its high intensity. The emission from the $^5\text{D}_0 \rightarrow ^7\text{F}_4$ transition can be also used; however, one should be aware of the overlap with the second harmonic at 700 nm (for 350 nm excitation). The excitation band of the $^7\text{F}_0 \rightarrow ^5\text{D}_4$ transition is observed at approximately 364 nm, while that of $^7\text{F}_0 \rightarrow ^5\text{L}_6$ is detected at approximately 395 nm, $^7\text{F}_0 \rightarrow ^5\text{D}_2$ – at 467 nm, and $^7\text{F}_0 \rightarrow ^5\text{D}_1$ – at 525 nm.
2. The intensities of the excitation bands must be integrated, and their barycentres should be determined. It is easier to obtain the barycentre wavelength (sometimes called a centroid), which is the centre of gravity of the transition peaks. In this case, the integrated intensities are equal to $\Gamma_2 = \Gamma(^7\text{F}_0 \rightarrow ^5\text{D}_2)$, $\Gamma_4 = \Gamma(^7\text{F}_0 \rightarrow ^5\text{D}_4)$, $\Gamma_6 = \Gamma(^7\text{F}_0 \rightarrow ^5\text{L}_6)$, and $\Gamma_{\text{MD}} = \Gamma(^7\text{F}_0 \rightarrow ^5\text{D}_1)$. The wavelength barycentres are denoted by symbol $\tilde{\lambda}$. Owing to the nature of the Eu^{3+} excitation spectrum, they are almost equal to the wavelengths of the peak maxima.
3. A refractive index value should be determined for each transition using the dispersion relation (if possible). For several hundred materials, dispersion relations are stored in a refractive index online database⁴⁵. The values of the refractive index are computed by the formulas $n_2 = n(467 \text{ nm})$, $n_4 = n(364 \text{ nm})$, $n_6 = n(395 \text{ nm})$, and $n_{\text{MD}} = n(525 \text{ nm})$.
4. The following three simplified equations can be used for parametrisation:

$$\Omega_2 = 7.803 \frac{n_2 n_{\text{MD}}}{(n_2^2 + 2)^2} \frac{\tilde{\lambda}_2}{\tilde{\lambda}_{\text{MD}}} \frac{\Gamma_2}{\Gamma_{\text{MD}}} \cdot 10^{-20} \text{cm}^2, \quad (18)$$

$$\Omega_4 = 6.384 \frac{n_4 n_{\text{MD}}}{(n_4^2 + 2)^2} \frac{\tilde{\lambda}_4}{\tilde{\lambda}_{\text{MD}}} \frac{\Gamma_4}{\Gamma_{\text{MD}}} \cdot 10^{-20} \text{cm}^2, \quad (19)$$

$$\Omega_6 = 0.459 \frac{n_6 n_{MD}}{(n_6^2 + 2)^2} \frac{\tilde{\lambda}_6}{\tilde{\lambda}_{MD}} \frac{\Gamma_6}{\Gamma_{MD}} \cdot 10^{-20} \text{cm}^2. \quad (20)$$

The developed parametrisation procedure is illustrated in Figure 2 (left) and compared with the Krupke method (right) using the Eu^{3+} emission spectrum.

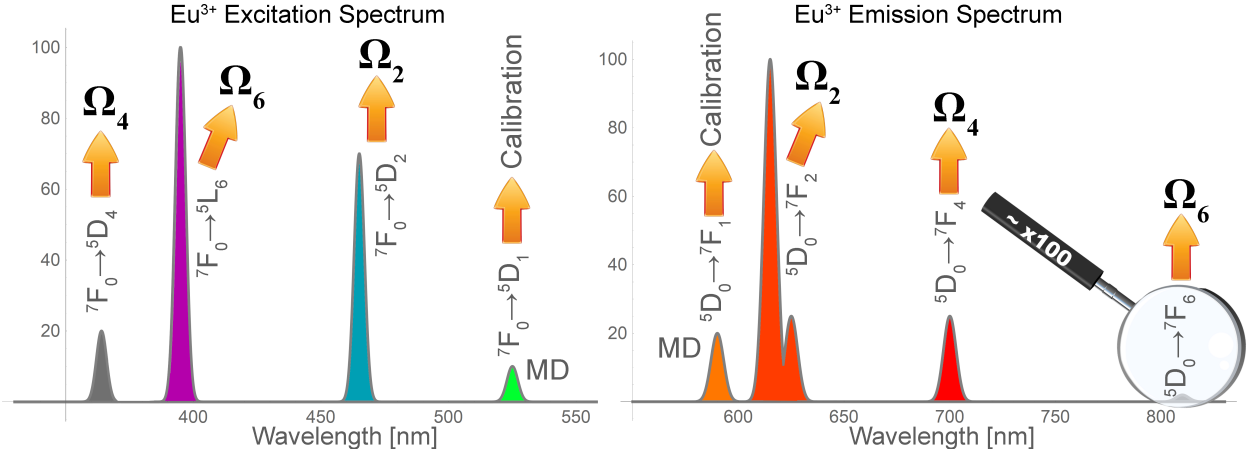


Figure 2 JO parametrisation schemes using the excitation and emission spectra of the Eu^{3+} ion: JOEX (left) and Krupke's method (right).

To facilitate the described procedure and make it universally accessible, a user-friendly web application for the JO parameter calculations via equations (18)–(20) was developed. It can be accessed at <https://omasgroup.org/judd-ofelt-from-excitation-spectrum-of-eu/> (Figure 3) and represents a free open-source web application written in PHP. After inputting the integrated intensities of the excitation bands of relevant transitions, their barycentre wavelengths, and refractive index values, the program outputs the calculated JO parameters.

Judd-Ofelt from Eu³⁺ excitation spectrum

The app is under GPLv3 license

1 Refractive index	2 Barycenter wavelengths [nm]	3 Integrated Intensities [a.u.]
n(364 nm) = <input type="text"/>	$\lambda(^5D_4)$ = <input type="text"/>	$I(^5D_4)$ = <input type="text"/>
n(397 nm) = <input type="text"/>	$\lambda(^5L_6)$ = <input type="text"/>	$I(^5L_6)$ = <input type="text"/>
n(465 nm) = <input type="text"/>	$\lambda(^5D_2)$ = <input type="text"/>	$I(^5D_2)$ = <input type="text"/>
n(526 nm) = <input type="text"/>	$\lambda(^5D_1)$ = <input type="text"/>	$I(^5D_1)$ = <input type="text"/>

Figure 3. Web application for calculating JO parameters from an excitation spectrum, which is available at <https://omasgroup.org/judd-ofelt-from-excitation-spectrum-of-eu/>.

5. Experimental verification of the JOEX method

For comparison, JO parameters were estimated from the emission spectrum of the Eu³⁺-activated Y₂SiO₅ microcrystalline phosphor and β -NaYF₄ nanoparticles using the JOES software⁴⁴. The relative deviation from the average value of the JO parameters obtained using the excitation ($\Omega_{\lambda}^{\text{ex}}$) and emission ($\Omega_{\lambda}^{\text{em}}$) spectra were calculated by the following formula⁴⁶:

$$\delta_{\lambda}[\%] = \left| 1 - \frac{2\Omega_{\lambda}^{\text{em}}}{\Omega_{\lambda}^{\text{em}} + \Omega_{\lambda}^{\text{ex}}} \right| \cdot 100\%. \quad (21)$$

4.1 Y₂SiO₄:Eu³⁺ microcrystalline powder

The emission and excitation spectra of Y₂SiO₄:Eu³⁺ are shown in Figure 4. The refractive index values of Y₂SiO₅ at the barycentre wavelengths of relevant transitions were calculated via the dispersion relation provided in Ref.⁴⁷. The parameters used for calculating JO parameters from the excitation spectrum (Figure 4b), JO parameters, and their deviations from the values estimated by utilising the emission spectrum (Figure 4a) are listed in Table 2.

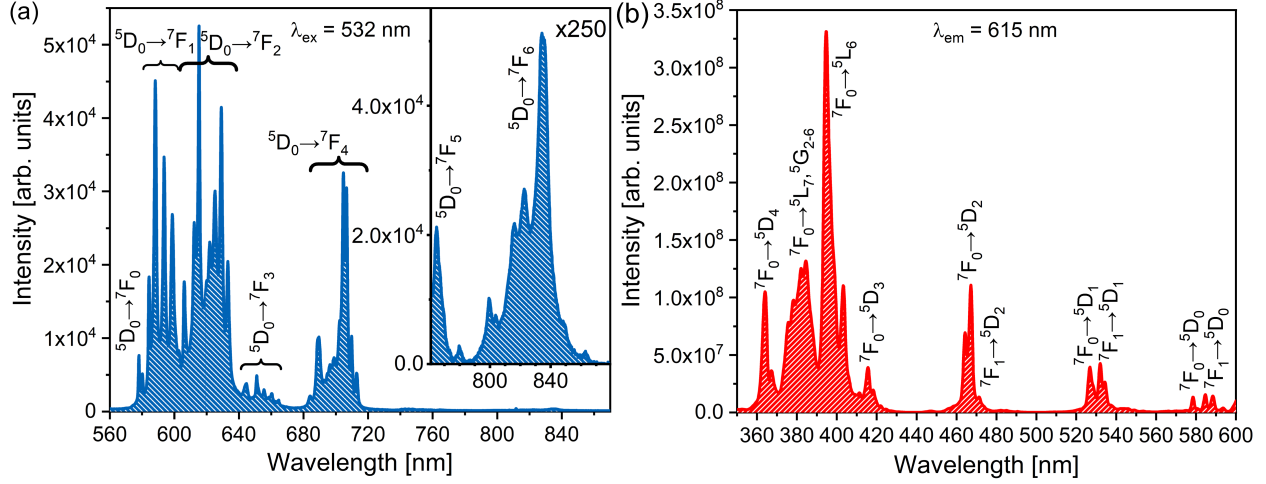


Figure 4. Emission spectrum of $Y_2SiO_5:Eu^{3+}$ obtained for the excitation to the 5L_6 level (a) its excitation spectrum obtained by monitoring the $^5D_0 \rightarrow ^7F_2$ emission (b).

Table 2. JO parameters determined from the excitation spectrum of $Y_2SiO_5:Eu^{3+}$ and their comparison with the values obtained from its emission spectrum.

λ	n	$\tilde{\lambda}_\lambda$ [nm]	$\Gamma_\lambda / \Gamma_{MD}$	$\Omega_\lambda^{ex} \cdot 10^{-20}$ [cm ²]	$\Omega_\lambda^{em} \cdot 10^{-20}$ [cm ²]	δ_λ [%]
2	1.809	465	3.34	2.731	2.745	0.3
4	1.795	364	3.49	1.847	2.347	11.9
6	1.799	397	15.69	0.649	0.661	0.9
MD	1.820	526				

The Ω_2 and Ω_6 values estimated by the excitation and emission parametrisation methods matched very well (the largest deviation of $\sim 12\%$ was obtained for the Ω_4 parameter).

4.2 β -NaYF₄:Eu³⁺ nanoparticles

The emission and excitation spectra of β -NaYF₄:Eu³⁺ are shown in Figure 5. The refractive index values were calculated using the Cauchy formula provided in Ref.⁴⁸, and the parametrisations data obtained from the spectra depicted in Figure 5 are presented in Table 3. Similar to the $Y_2SiO_5:Eu^{3+}$ parameters, the resulting $\Omega_{2,6}$ values are very close to each other, while the Ω_4 magnitudes differ by 13%.

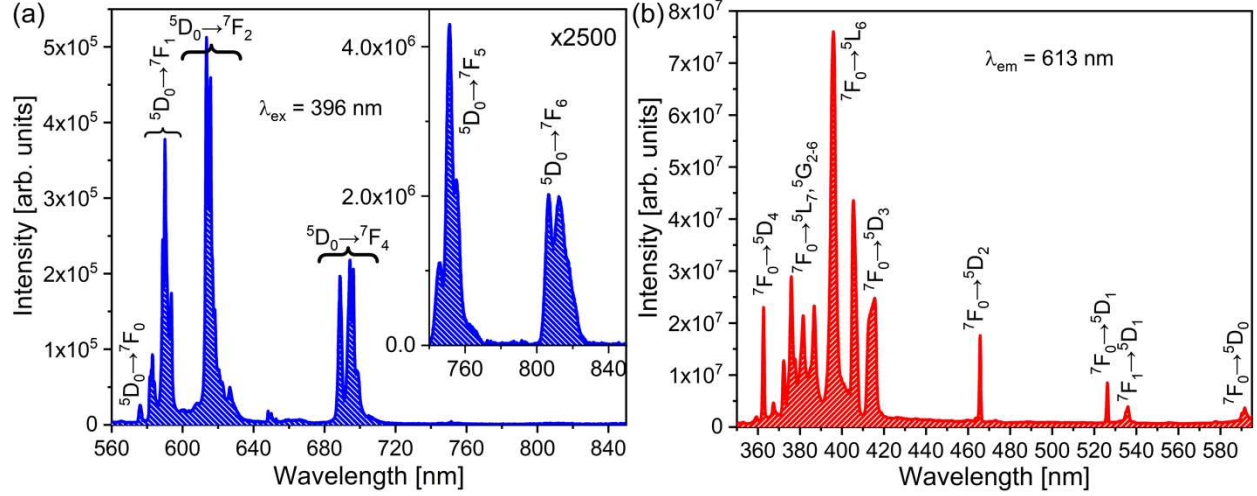


Figure 5. Emission spectrum of β -NaYF₄:Eu³⁺ obtained for the excitation to the ⁵L₆ level (a) its excitation spectrum obtained by monitoring the ⁵D₀→⁷F₂ emission (b).

Table 3. JO parameters estimated from the excitation spectrum of β -NaYF₄:Eu³⁺.

λ	n	$\tilde{\lambda}_\lambda$ [nm]	$\Gamma_\lambda / \Gamma_{MD}$	$\Omega_\lambda^{ex} \cdot 10^{-20}$ [cm ²]	$\Omega_\lambda^{em} \cdot 10^{-20}$ [cm ²]	δ_λ [%]
2	1.493	466	2.66	2.28	2.13	3.4
4	1.540	362	2.40	1.26	0.97	13.0
6	1.513	398	35.59	1.51	1.62	3.5
MD	1.483	526				

6. Conclusion

In this study, we developed a comprehensive self-referenced method for estimating all JO intensity parameters of Eu³⁺-doped compounds from their excitation spectra. Compared to the parametrisation of absorption spectra, the proposed technique is more accurate and can be applied to any material form. In addition, this method is self-calibrated and requires no additional measurements apart from a single excitation spectrum.

The accuracy and suitability of the described approach were experimentally verified for phosphors with different chemical compositions and morphologies. Excellent matching of the obtained Ω_2 and Ω_6 parameters was observed with a slight difference between the Ω_4 values

whose origin has not been established yet. The proposed method facilitates a simple derivation of Ω_6 intensity parameters, which are difficult to calculate by the parametrisation of emission spectra and, therefore, frequently omitted in related studies.

One should note that the presented work is not extending the JO theory to explain its shortcomings but provides a new theoretical and computational tool for its practices. For an easier, faster, and reliable computational procedure, we have also developed a special web application available at <https://omasgroup.org/judd-ofelt-from-excitation-spectrum-of-eu/>. The direction of future work is the calculation of JO intensity parameters for many important phosphors for which available parametrisation approaches were not feasible or sufficiently precise.

Acknowledgments

This research was funded by the Ministry of Education, Science, and Technological Development of the Republic of Serbia.

Author Contributions

All authors have equal contribution.

Data Availability Statement

Data are available from Aleksandar Ćirić upon a reasonable request.

Competing interests

The authors declare no conflicts of interest.

References

1. Zhou, B., Li, Z. & Chen, C. Global potential of rare earth resources and rare earth demand from clean technologies. *Minerals* **7**, 203 (2017). <https://doi.org/10.3390/min7110203>.
2. Tukker, A. Rare earth elements supply restrictions: Market failures, not scarcity, hamper their current use in high-tech applications. *Environ. Sci. Technol.* **48**, 9973–9974 (2014). <https://doi.org/10.1021/es503548f>.
3. Liu, G. & Jacquier, B. (eds). *Spectroscopic Properties of Rare Earths in Optical Materials* (Springer-Verlag, Berlin/Heidelberg, 2005). <https://doi.org/10.1007/3-540-28209-2>.
4. Van Vleck, J. H. The puzzle of rare-earth spectra in solids. *J. Phys. Chem.* **41**, 67–80 (1937). <https://doi.org/10.1021/j150379a006>.
5. Walsh, B. M. Judd–Ofelt theory: Principles and practices. In: *Advances in Spectroscopy for Lasers and Sensors*, (eds Di Bartolo, B. & Forte, O.) 403–433 (Springer, Netherlands, Dordrecht, 2006). https://doi.org/10.1007/1-4020-4789-4_21.
6. Judd, B. R. Optical absorption intensities of rare-earth ions. *Phys. Rev.* **127**, 750–761 (1962). <https://doi.org/10.1103/PhysRev.127.750>.
7. Ofelt, G. S. Intensities of crystal spectra of rare-earth ions. *J. Chem. Phys.* **37**, 511–520 (1962). <https://doi.org/10.1063/1.1701366>.
8. Wybourne, B. G. The fascination of the rare earths – then, now and in the future. *J. Alloys Compd.* **380**, 96–100 (2004). <https://doi.org/10.1016/j.jallcom.2004.03.034>.
9. Hehlen, M. P., Brik, M. G. & Krämer, K. W. 50th anniversary of the Judd–Ofelt theory: An experimentalist’s view of the formalism and its application. *J. Lumin.* **136**, 221–239

- (2013). <https://doi.org/10.1016/j.jlumin.2012.10.035>.
10. Smentek, L. Judd-Ofelt theory – the golden (and the only one) theoretical tool of f-electron spectroscopy. In: *Computational Methods in Lanthanide and Actinide Chemistry Ch 10* (ed Dolg, M.) 241–268 (John Wiley & Sons Ltd, Chichester, UK, 2015). <https://doi.org/10.1002/9781118688304.ch10>.
 11. Goldner, P. & Auzel, F. Application of standard and modified Judd–Ofelt theories to a praseodymium-doped fluorozirconate glass. *J. Appl. Phys.* **79**, 7972–7977 (1996). <https://doi.org/10.1063/1.362347>.
 12. Ćirić, A., Ristić, Z., Barudzija, T., Srivastava, A. & Dramićanin, M. D. Judd–Ofelt parametrization from the emission spectrum of Pr³⁺ doped materials: Theory, application software, and demonstration on Pr³⁺ doped YF₃ and LaF₃. *Adv. Theory Simulations* **4**, 2100082 (2021). <https://doi.org/10.1002/adts.202100082>.
 13. Sytsma, J., Imbusch, G. F. & Blasse, G. The spectroscopy of Gd³⁺ in yttriumoxychloride: Judd–Ofelt parameters from emission data. *J. Chem. Phys.* **91**, 1456–1461 (1989). <https://doi.org/10.1063/1.457106>.
 14. Yao, G., Lin, C., Meng, Q., Stanley May, P. & Berry, M. T. Calculation of Judd–Ofelt parameters for Er³⁺ in β-NaYF₄: Yb³⁺, Er³⁺ from emission intensity ratios and diffuse reflectance spectra. *J. Lumin.* **160**, 276–281 (2015). <https://doi.org/10.1016/j.jlumin.2014.12.025>.
 15. Luo, W., Liao, J., Li, R. & Chen, X. Determination of Judd–Ofelt intensity parameters from the excitation spectra for rare-earth doped luminescent materials. *Phys. Chem. Chem. Phys.* **12**, 3276–3282 (2010). <https://doi.org/10.1039/b921581f>.

16. Ćirić, A., Stojadinović, S., Brik, M. G. & Dramićanin, M. D. Judd–Ofelt parametrization from emission spectra: The case study of the $\text{Eu}^{3+} \ ^5\text{D}_1$ emitting level. *Chem. Phys.* **528**, 110513 (2020). <https://doi.org/10.1016/j.chemphys.2019.110513>.
17. Krupke, W. F. Optical absorption and fluorescence intensities in several rare-earth-doped Y_2O_3 and LaF_3 single crystals. *Phys. Rev.* **145**, 325–337 (1966). <https://doi.org/10.1103/PhysRev.145.325>.
18. Görrler-Walrand, C. & Binnemans, K. Chapter 167. Spectral intensities of f–f transitions. *Handbook on the Physics and Chemistry of Rare Earths* **25**, 101–264 (1998). [https://doi.org/10.1016/S0168-1273\(98\)25006-9](https://doi.org/10.1016/S0168-1273(98)25006-9).
19. Ćirić, A., Stojadinović, S. & Dramićanin, M. D. An extension of the Judd–Ofelt theory to the field of lanthanide thermometry. *J. Lumin.* **216**, 116749 (2019). <https://doi.org/10.1016/j.jlumin.2019.116749>.
20. Ćirić, A., Stojadinović, S. & Dramićanin, M. D. Approximate prediction of the CIE coordinates of lanthanide-doped materials from the Judd–Ofelt intensity parameters. *J. Lumin.* **213**, 395–400 (2019). <https://doi.org/10.1016/j.jlumin.2019.05.052>.
21. Dejneka, M., Snitzer, E. & Riman, R. E. Blue, green and red fluorescence and energy transfer of Eu^{3+} in fluoride glasses. *J. Lumin.* **65**, 227–245 (1995). [https://doi.org/10.1016/0022-2313\(95\)00073-9](https://doi.org/10.1016/0022-2313(95)00073-9).
22. Ćirić A., Zeković, I., Medić, M., Antić, Ž. & Dramićanin, M. D. Judd–Ofelt modelling of the dual-excited single band ratiometric luminescence thermometry. *J. Lumin.* **225**, 117369 (2020). <https://doi.org/10.1016/j.jlumin.2020.117369>.

23. Carnall, W. T., Crosswhite, H. & Crosswhite, H. M. Energy level structure and transition probabilities in the spectra of the trivalent lanthanides in LaF₃, Argonne, IL (United States), 1978. <https://doi.org/10.2172/6417825>.
24. Ćirić, A., Gavrilović, T. & Dramićanin, M. D. Luminescence intensity ratio thermometry with Er³⁺: Performance overview. *Crystals* **11**, 189 (2021). <https://doi.org/10.3390/cryst11020189>.
25. Dodson, C. M. & Zia, R. Magnetic dipole and electric quadrupole transitions in the trivalent lanthanide series: Calculated emission rates and oscillator strengths. *Phys. Rev. B* **86**, 125102 (2012). <https://doi.org/10.1103/PhysRevB.86.125102>.
26. Toptygin, D. Effects of the solvent refractive index and its dispersion on the radiative decay rate and extinction coefficient of a fluorescent solute. *J. Fluoresc.* **13**, 201–219 (2003). <https://doi.org/10.1023/A:1025033731377>.
27. Dutra, J. D. L., Bispo, T. D. & Freire, R. O. LUMPAC lanthanide luminescence software: Efficient and user friendly. *J. Comput. Chem.* **35**, 772–775 (2014). <https://doi.org/10.1002/jcc.23542>.
28. Smentek, L., Wybourne, B. G. & Hess, B. A. Judd–Ofelt theory in a new light on its (almost) 40th anniversary. *J. Alloys Compd.* **323–324**, 645–648 (2001). [https://doi.org/10.1016/S0925-8388\(01\)01185-9](https://doi.org/10.1016/S0925-8388(01)01185-9).
29. Malta, O. L. & Carlos, L. D. Intensities of 4f–4f transitions in glass materials. *Quim. Nova* **26**, 889–895 (2003). <https://doi.org/10.1590/S0100-40422003000600018>.
30. Wen, J. et al. Ab-initio calculations of Judd–Ofelt intensity parameters for transitions

- between crystal-field levels. *J. Lumin.* **152**, 54–57 (2014).
<https://doi.org/10.1016/j.jlumin.2013.10.055>.
31. Xue, S. D., Liu, M. H., Zhang, P., Wong, W. H. & Zhang, D. L. Validity of Judd–Ofelt spectroscopy based on diffuse reflectance spectrum and fluorescence lifetime of phosphor. *J. Lumin.* **224**, 117304 (2020). <https://doi.org/10.1016/j.jlumin.2020.117304>.
 32. Binnemans, K. Interpretation of europium(III) spectra. *Coord. Chem. Rev.* **295**, 1–45 (2015). <https://doi.org/10.1016/j.ccr.2015.02.015>.
 33. Moret, E., Bünzli, J. C. G. & Schenk, K. J. Structural and luminescence study of europium and terbium nitrate hexahydrates. *Inorganica Chim. Acta* **178**, 83–88 (1990).
[https://doi.org/10.1016/S0020-1693\(00\)88138-4](https://doi.org/10.1016/S0020-1693(00)88138-4).
 34. Hopkins, T. A., Bolender, J. P., Metcalf, D. H. & Richardson, F. S. Polarized optical spectra, transition line strengths, and the electronic energy-level structure of $\text{Eu}(\text{dpa})_3^{3-}$ complexes in single crystals of hexagonal $\text{Na}_3[\text{Yb}_{0.95}\text{Eu}_{0.05}(\text{dpa})_3] \cdot \text{NaClO}_4 \cdot 10\text{H}_2\text{O}$. *Inorg. Chem.* **35**, 5347–5355 (1996). <https://doi.org/10.1021/ic951524g>.
 35. Babu, P. & Jayasankar, C. K. Optical spectroscopy of Eu^{3+} ions in lithium borate and lithium fluoroborate glasses. *Phys. B Condens. Matter* **279**, 262–281 (2000).
[https://doi.org/10.1016/S0921-4526\(99\)00876-5](https://doi.org/10.1016/S0921-4526(99)00876-5).
 36. Lavín, V., Rodríguez-Mendoza, U. R., Martín, I. R. & Rodríguez, V. D. Optical spectroscopy analysis of the Eu^{3+} ions local structure in calcium diborate glasses. *J. Non. Cryst. Solids* **319**, 200–216 (2003). [https://doi.org/10.1016/S0022-3093\(02\)01914-2](https://doi.org/10.1016/S0022-3093(02)01914-2).
 37. Chen, X. Y. & Liu, G. K. The standard and anomalous crystal-field spectra of Eu^{3+} . *J.*

- Solid State Chem.* **178**, 419–428 (2005). <https://doi.org/10.1016/j.jssc.2004.09.002>.
38. Silva, G. H. et al. Eu³⁺ emission in phosphate glasses with high UV transparency. *J. Lumin.* **154**, 294–297 (2014). <https://doi.org/10.1016/j.jlumin.2014.04.043>.
39. Alqarni, A. S. et al. Intense red and green luminescence from holmium activated zinc-sulfo-boro-phosphate glass: Judd–Ofelt evaluation. *J. Alloys Compd.* **808**, 151706 (2019). <https://doi.org/10.1016/j.jallcom.2019.151706>.
40. Jørgensen, C. K. & Reisfeld, R. Judd–Ofelt parameters and chemical bonding. *J. Less Common Met.* **93**, 107–112 (1983). [https://doi.org/10.1016/0022-5088\(83\)90454-X](https://doi.org/10.1016/0022-5088(83)90454-X).
41. Denault, K. A. et al. Average and local structure, Debye temperature, and structural rigidity in some oxide compounds related to phosphor hosts. *ACS Appl. Mater. Interfaces* **7**, 7264–7272 (2015).
42. Zhuo, Y., Mansouri Tehrani, A., Oliynyk, A. O., Duke, A. C. & Brgoch, J. Identifying an efficient, thermally robust inorganic phosphor host via machine learning. *Nat. Commun.* **9**, 4377 (2018). <https://doi.org/10.1038/s41467-018-06625-z>.
43. Mason, S. F., Peacock, R. D. & Stewart, B. Dynamic coupling contributions to the intensity of hypersensitive lanthanide transitions. *Chem. Phys. Lett.* **29**, 149–153 (1979). [https://doi.org/10.1016/0009-2614\(74\)85001-3](https://doi.org/10.1016/0009-2614(74)85001-3).
44. Ćirić, A., Stojadinović, S., Sekulić, M. & Dramićanin, M. D. JOES: An application software for Judd–Ofelt analysis from Eu³⁺ emission spectra. *J. Lumin.* **205**, 351–356 (2019). <https://doi.org/10.1016/j.jlumin.2018.09.048>.
45. Polyanskiy, M. N. Refractive Index Database (n.d.). <https://refractiveindex.info> (accessed

on March 5, 2018).

46. Weisstein, E. W. Relative Deviation, MathWorld – A Wolfram Web Resource (n.d.). <https://mathworld.wolfram.com/RelativeDeviation.html> (accessed on August 5, 2021).
47. Beach, R., Shinn, M. D., Davis, L., Solarz, R. W. & Krupke, W. F. Optical absorption and stimulated emission of neodymium in yttrium orthosilicate. *IEEE J. Quantum Electron.* **26**, 1405–1412 (1990). <https://doi.org/10.1109/3.59689>.
48. Sokolov, V. I. et al. Determination of the refractive index of β -NaYF₄/Yb³⁺/Er³⁺/Tm³⁺ nanocrystals using spectroscopic refractometry. *Opt. Spectrosc.* **118**, 609–613 (2015). <https://doi.org/10.1134/S0030400X15040190>.